

Occurrence of two-stage hardening in C-Mn steel wire rods containing pearlitic microstructure

Balbir Singh, Gadadhar Sahoo and Atul Saxena

Steel Authority of India limited, R&D Centre for Iron and Steel, Ranchi, Jharkhand, India

Abstract: The 8 and 10 mm diameter wire rods intended for use as concrete reinforcement were produced/ hot rolled from C-Mn steel chemistry containing various elements within the range of C:0.55-0.65, Mn:0.85-1.50, Si:0.05-0.09, S:0.04 max, P:0.04 max and N:0.006 max wt%. Depending upon the C and Mn contents the product attained pearlitic microstructure in the range of 85-93% with balance amount of polygonal ferrite transformed at prior austenite grain boundaries. The pearlitic microstructure in the wire rods helped in achieving yield strength, tensile strength, total elongation and reduction in area values within the range of 422-515 MPa, 790-950 MPa, 22-15% and 45-35%, respectively. On analyzing the tensile results it was revealed that the material experienced hardening in two stages separable by a knee strain value of about 0.05. The occurrence of two stage hardening thus in the steel with hardening coefficients of 0.26 and 0.09 could be demonstrated with the help of derived relationships existed between flow stress and the strain.

1. Introduction

As it is known, carbon and manganese are the basic elements which control strength and ductility in C-Mn steels. Besides, the final microstructure in the product also plays an important role in contributing to these parameters and the mechanism of deformation. As the steels containing carbon and manganese are expected to have ferrite-pearlite microstructure just after hot rolling and normal industrial cooling, the volume fraction and lamellar spacing of pearlite strongly influence the deformation mechanism [1-2]. The cementite and the ferrite components of the lamellar structure having marginally different strength levels exhibit different strain hardening levels due to formation of more ordered dislocation sub-structures during deformation. The strain hardening of both the components at different strain levels thus gives rise to two-stage hardening behavior or double 'n' effect in the pearlitic steels. In the present study an attempt has been made to demonstrate this phenomenon with the help of a conventional tensile test conducted on a C-Mn structural steel wire rod containing C and Mn in the ranges of 0.55-0.65 and 0.85-1.50, respectively. Apart from the tensile test the material was subjected to optical microscopy, hardness measurements, bend test and scanning electron microscopic observations of the fractured surface.

2. Experimental

2.1. Material

The experimental wire rods for the present study were manufactured with desired end properties by considering the shop logistics such as steel making, rolling and cooling practices at Bhilai Steel Plant. Accordingly, five number of semi-killed steel heats were made in the basic open hearth furnace



(BOH), wherein sulphur and phosphorous levels could be controlled to less than 0.04%. It was also understood that nitrogen contents lower than 40 to 60 ppm were easily attainable in the BOH. The molten steel thus made, was poured into 8 ton ingot moulds using top pouring practice. The solidified ingots obtained on stripping were hot charged into soaking pits with minimum temperature being about 700°C. Heating upto 850°C was at a rate of ~50°C/ hour and thereafter faster, upto 1300°C. The ingots were homogenized at this temperature for 6 hours and subsequently fed to the blooming and billet mill wherein they were rolled into 400 mm square blooms in 15 to 17 passes. The front and the back ends were cropped using a 1000 ton shear. Subsequently, the blooms were rolled to 85 mm square billets of 12 meter length in the continuous billet mill.

The billets, thus obtained, were charged into reheating furnaces wherein a temperature of 1170°C was maintained at the front end and 1220°C at the back end. After soaking for about one and half hour the billets were rolled in four strand continuous wire rod mill to 8 and 10 mm diameter rods. The temperature during rolling was maintained in the range of 1000-1150°C while the rolling was completed at about 950-1000°C by controlling the finish rolling speed to about 20 meter per second. To achieve adequate bond strength of reinforcement in the concrete, a specially designed rib pattern was made on the rod surface in the last finishing stand. After finish rolling the wire rods were coiled and subsequently cooled on the hook conveyors. Samples for various tests were collected from the coils after they had cooled down to ambient temperature.

2.2. Optical Metallography

In order to examine the microstructure, specimens of about 10 mm height were cut from both the 8 mm and the 10 mm diameter rods. Subsequently, the cut specimens were mounted using a hot mount press. The mounted specimens were ground and paper polished in the usual manner upto 600 grit. Final polishing was done on a wheel cloth with 0.1 micron alumina solution as abrasive. After polishing, the specimens were rinsed in soap solution thoroughly and dried before further etching with a freshly prepared 2% nital solution. The specimens thus prepared, were observed under Neophot-30 optical microscope and microstructures photographed at desired magnifications.

2.3. Hardness Measurements

Hardness measurements were carried out on transverse sections cut from the wire rods in the as-received condition. The cut section of about 10 mm height was ground to about 1 mm depth and subsequently paper polished upto 600 grit. Hardness measurements were carried out on a Vicker's hardness tester at 20 kg load across the diameter. While measuring ocular readings an average of both the diagonals of the indentation was taken.

2.4. Tensile Testing

Tensile tests were conducted in INSTRON-1195 static model universal testing machine. For obtaining the yield strength, tensile strength, percent elongation and percent reduction in area of the as-rolled wire rods, specimens were tested without machining because as per the standard round structurals including reinforcement bars and wire rods up to 25 mm diameter are to be tested without reducing their cross-sectional area. During each test a cross-head speed of 1 mm/minute was maintained and load-elongation curve plotted on an X-Y plotter. A minimum of three specimens for each lot were tested and average value of the properties obtained.

To assess the work hardening characteristics of the experimental wire rods, tests were conducted on the machined specimens. The sub-sized round specimens having 25 mm gauge length and 6.25 mm gauge diameter were fabricated as per ASTM: A-6 specification. During the tests a strain rate of 2.4s^{-1} was employed and actual increments in the gauge length were recorded using a 25 mm strain gauge/ extensometer.

2.5. Bend Test

In order to assess the ductility of the material, bend test is conducted around a mandrel of specified diameter. Three point bend fixture with 25 mm diameter roller was used in INSTRON-1195 machine for bending reinforcement wire rods, hot-rolled from C-Mn chemistry, at a cross-head speed of 2 mm/minute. The 300 mm long sample was bent around a mandrel of 3d (where 'd' is the nominal diameter of rod) as specified in BIS:1786 specification [3]. After the bar/wire rod was bent around 180° it was taken out of the machine and the bent surface was observed visually for surface cracks, if any.

2.6. Scanning Electron Microscopy

To identifying the mode of fracture in tensile tested specimens, fractured surfaces of C-Mn rods were observed under SEM-JSM 840A scanning electron microscope. Prior to loading the specimen inside the SEM chamber, fractured portion of the tensile tested specimen was cut to the required size and cleaned ultrasonically with acetone. During observations, SEM operation was set to the secondary electron mode at an accelerating voltage of 20 KV. The type of fracture, whether dimpled or cleavage, was recorded in the form of photographs at appropriate magnification.

3.0 Results

3.1. Chemical composition

Chemical composition of all the experimental heats as determined through optical emission spectroscopy is given in Table 1. It may be seen from the table that all the five heats contained amounts of C, Mn, Si, P and S within the desired range. Carbon equivalent was also calculated for these chemistries which varied between 0.69-0.86.

Table 1. Chemical composition of the C-Mn steel wire rods

Heat No.	Rolled Diameter (mm)	Chemical Composition (wt.%)						
		C	Mn	Si	S	P	N	Al
1	10	0.55	0.85	0.08	0.017	0.030	0.005	0.02
2	8	0.58	0.95	0.06	0.028	0.040	0.004	0.03
3	10	0.59	1.50	0.05	0.021	0.045	0.004	0.03
4	10	0.63	1.35	0.06	0.036	0.032	0.005	0.04
5	8	0.65	1.25	0.09	0.027	0.035	0.004	0.02

3.2. Microstructure

Microstructure of C-Mn steel wire rods produced through normal processing route comprised lamellar pearlite and proeutectoid ferrite present along prior austenite grain boundaries (Figure 1).



Figure 1. Microstructure of C-Mn wire rods

Since the carbon and manganese contents in the experimental heats varied over a narrow range, there was not much variation in the amounts of the two microconstituents, i.e. ferrite and pearlite. As shown in Table 2, the pearlite content varied between 80-93% with the balance being ferrite. The pearlite

formed in the steel was fine and had an inter-lamellar spacing in the range of 0.2-0.6 μm as measured through the line intersection method. Prior austenite grain size was also estimated, which varied between 28-40 μm . Out of the five heats, microstructure of heat # 4 comprised evenly distributed fine pearlitic grains (size $\sim 28 \mu\text{m}$) interspersed with grain boundary ferrite. This was not so with the other heats (Figure 1).

Table 2. Volume fraction of constituents in C-Mn steel

Heat No.	Rolled Dia. (mm)	Carbon Equivalent	Pearlite (%)	Ferrite (%)	Hardness (Hv20)
1	10	0.69	90	10	257
2	8	0.74	85	15	280
3	10	0.84	93	7	286
4	10	0.86	80	20	294
5	8	0.86	92	8	289

3.3. Hardness

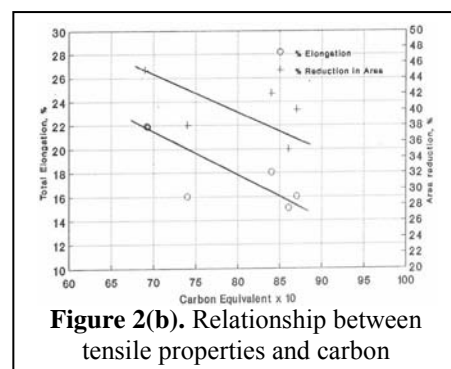
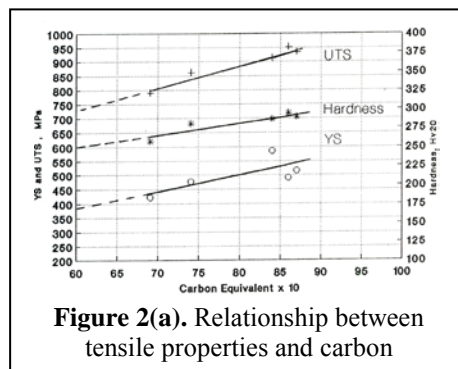
Hardness values measured on the specimens from all the five heats are given in Table 3. It may be seen from the table that hardness was found to vary between 257 to 294 Hv and increased with CE in a manner similar to the tensile strength. Since a relationship exists between tensile strength and hardness, the data pertaining to them were analyzed and it emerged that the two are related through a relationship of the form: $\text{UTS (MPa)} = 4.42 \text{ Hv} - 354$

Table 3. Tensile properties and hardness of as hot rolled C-Mn steel wire rods.

Heat No.	Rolled Diameter (mm)	Carbon Equivalent (%)	YS (MPa)	UTS (MPa)	T.El (%)	Reduction in Area (%)	YS/UTS Ratio	Hardness (Hv20)
1	10	0.69	422	790	22	45	0.53	257
2	8	0.74	476	862	19	38	0.55	280
3	10	0.84	585	913	18	42	0.64	286
4	10	0.86	490	952	15	35	0.52	294
5	8	0.86	515	933	16	40	0.55	289

3.4. Tensile Properties

Yield strength, tensile strength, % elongation and % reduction in area of 8 and 10 mm dia. as-rolled wire rods were evaluated from the load-elongation data and are reported in Table 3. It is seen from this table that YS varied between 422 to 585 MPa, UTS between 790 to 952 MPa, %TEL between 16 to 22 and % reduction in area between 35 to 45. YS/UTS ratio was computed to be in the range of 0.52 to 0.64. The values thus obtained were plotted against the carbon equivalent of steels (Figures 2a&b) to assess the combined effect of carbon and manganese contents. It emerged that as CE increased YS and the UTS also increased while %TEL and %RA decreased almost linearly.



If it is assumed that the carbon equivalent for the heats # 3 & 4 (0.84 & 0.86 respectively) are nearly identical the mechanical properties data summarized in Table 3 and Figures 2(a&b) can be interpreted a little further. It clearly emerges that the presence of relatively lower carbon and higher Mn contents (as in heat # 3) has resulted in better overall mechanical properties than what is obtained in heat # 4 with a higher carbon and relatively lower Mn content.

Analyzing the engineering stress-strain data through computational techniques for the specimen from heat # 3 proved helpful in arriving at the true stress-strain values which were plotted on log-log scale (Figure 3). Work hardening rate ($\partial\sigma/\partial\epsilon$) for this specimen was also computed and plotted against true strain as shown in Figure 4. Through regression analysis, work hardening parameters 'n' and 'K' were also calculated with a determination index of 0.999.

The plot in Figure-3 has two slopes revealing the strain hardening to be occurring in two-stages (double-n effect). The first stage hardening is observed upto a true strain of about 0.05 and second stage beyond this limit. It is, therefore, deduced that 0.05 is the critical strain [4] or knee strain for the present steel (heat # 3). Hardening exponent ' n_1 ' and hardening coefficient ' k_1 ' for the first stage have been computed as 0.26 and 1715 MPa while for second stage, ' n_2 ' and ' k_2 ' were estimated to be 0.09 and 1065 MPa, respectively.

Thus, for the experimental steel the power law relationships can be expressed as :

$$\begin{aligned}\sigma_1 &= 1715 \epsilon^{0.26} && \text{for } \epsilon \leq 0.05, \text{ knee strain} - 1^{\text{st}} \text{ stage hardening} \\ \sigma_2 &= 1065 \epsilon^{0.09} && \text{for } \epsilon > 0.05, \text{ knee strain} - 2^{\text{nd}} \text{ stage hardening}\end{aligned}$$

Thus, during tensile loading, the material (C-Mn steel) behaved in accordance with the following model:

$$\begin{aligned}\sigma &= 1715 \epsilon^{0.26} && (\text{for } \epsilon \leq 0.05 \text{ knee strain}) \\ &= 1065 \epsilon^{0.09} && (\text{for } \epsilon > 0.05)\end{aligned}$$

On referring to Figure 4 it emerged that the rate of hardening in the material increased initially upto a strain level of about 0.03 and thereafter decreased. On approaching a strain level of 0.05 another peak, although comparatively smaller as compared to the previous one, was observed followed by a level off value beyond 0.08 strain.

3.5. Bending

Bending operation is one of the important requirements for steel rods used as reinforcements in concrete structures. This operation allows the wire rods to be hooked up with one another where welding is not a mandatory requirement for joining. Accordingly, 8 and 10 mm dia. experimental rods were bent through 180° around a mandrel of 3d (where 'd' is the diameter of rod) as per the norms laid down in BIS:1786 specification [3]. Inspection of the bent surfaces revealed that

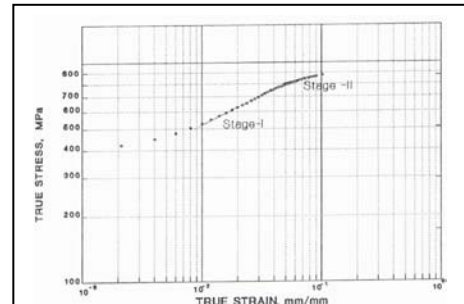


Figure 3. Log-Log plot of true stress-strain depicting two stages of strain hardening

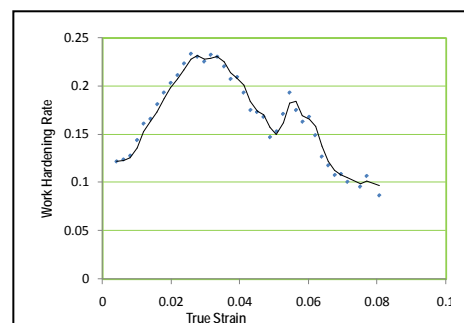


Figure 4. Plot depicting occurrence of two work hardening rates ($\partial\sigma/\partial\epsilon$).

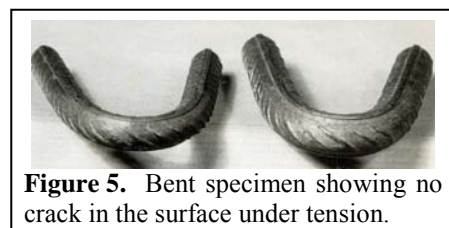


Figure 5. Bent specimen showing no crack in the surface under tension.

no cracks were visible even on the outer surface experiencing maximum tensile strains. Bent specimens of the two rods, from heat # 5 and 1 are shown in Figure 5.

3.6. Fractography

The fractographs as observed under SEM for the surface of the tensile tested broken specimen are depicted in Figures 6(a&b). From the SEM fractographs it emerged that specimens from all the heats showed cup and cone type of fracture which indicated that the experimental material is ductile (Figure 6a). This was confirmed by dimples present in the fractograph taken at higher magnification for the fractured steel (Figure 6b). However, in heat # 5 where C & Mn contents were relatively higher the fracture appearance was not fully ductile.

4.0 Discussion

It is understood that the end properties in materials are known to be a function of the chemical composition, the reheating, rolling and cooling parameters. Therefore, due precaution was taken to maintain these parameters within specified limits to meet with the property stipulations contained in BIS:1786 specification. The parameters of interest were accordingly varied right from the steel making stage down to cooling after finish rolling to ensure that the desired objectives were achieved.

Chemical composition of the experimental steel (Table 1) revealed that in all the five heats elements are present within the specified limits as envisaged during the alloy design. This was made possible through close monitoring of the blowing parameters and teeming practice followed in basic open hearth steel making at the Bhilai Steel Plant. The chemical composition, in combination with the prevailing rolling practice and cooling parameters was found to be helpful in obtaining the microstructure of interest, i.e. fine pearlite.

Soaking the steel ingots at 1300°C for 6 hours ensured homogenization vis-a-vis C and Mn atoms. This resulted into a reasonably homogeneous distribution of various elements in the billets which were the input material for producing wire rods. Similarly, reheating at ~1200°C for ~1½ hours ensured that the said temperature was unfailingly attained within the centre of billets prior to the onset of rolling. On subsequent rolling between 1000-1150°C fine austenite was obtained through a combination of deformation and recrystallization taking place due to multi-pass rolling practice. Finish rolling between 950-1000°C was sufficient to promote recrystallisation of deformed austenite grains even after the last finishing pass. A fine prior austenite grain size in the range of 28-40 µm was a result of concurrent deformation of austenite occurring during rolling in the roughing and finishing stands. After coiling, the wire rods were cooled at a rate of ~1°C/sec. as practiced at the Bhilai Steel Plant. This rate was found to be sufficient to produce a fine pearlitic microstructure containing a little amount of boundary ferrite [5,6]. Attainment of this microstructure is consistent with the chemical composition of the experimental material.

Tensile results revealed that the pearlitic microstructure produced high strengths and adequate ductility in as-rolled wire rods (Table 3). This is on account of a microstructure comprising fine pearlite. As per BIS:1786 the stipulated properties for the Fe₄₁₅ grade are ; YS 415 MPa, UTS 500 MPa and elongation 14.5%. This level of yield strength could be attained in the experimental steel at a carbon equivalent of ~0.65 as derived through extrapolation (Figure 2a). Tensile strength of ~780 MPa and elongation of ~20 % are attainable in the material at this carbon equivalent. It is thus inferred that the developed steel stands to satisfy the requirements of the aforementioned specification without any difficulty. The increase in tensile strength, hardness and yield strength with carbon equivalent is as per

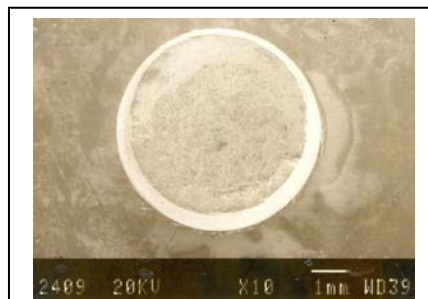


Figure 6(a). Cup and cone fracture in tensile tested specimen.

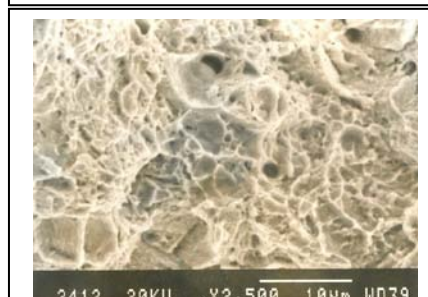


Figure 6(b). Dimpled ductile fracture in tensile tested specimen

expectations (Figure 2a and Table 3). An increase in hardness / strength decreases ductility as has been observed (Figure 2b and Table 3). The steep fall in ductility (Figure 2b) is because of crack sensitive nature of lamellar pearlite morphology.

Commenting upon the observation that for a given carbon equivalent a higher Mn and a lower C combination may be a better option than vice-versa in controlling tensile properties, it is pertinent to observe that a higher Mn and lower C combination appears better since the embrittling response is lesser. This can be further explained by stating that while Mn improves properties by refining grain size (thus improving ductility & toughness) and lowers the A_1 temperature (thereby refining pearlite), an increase in the carbon content, despite lowering A_1 , impairs ductility / toughness due to a larger solution hardening effect and an increase in the amount of pearlite.

This analysis could be further extended by stating that for attaining C equivalent of 0.65 (to meet with the requirements of BIS:1786 specification), we can either use 0.55%C and 0.60%Mn or 0.51%C and 0.85%Mn. The latter option would prove to be more useful provided it is ensured that the volume fraction of pearlite is within the range ~83-90%.

In addition to high strengths it further emerged that the material sustained higher amounts of strains (~0.10) before the onset of necking (Figure 3). A YS/UTS ratio of 0.52 to 0.64 indicated that the material has a high rate of work hardening. A work hardening exponent of 0.26, as computed through Hollomon power law relationship, also pointed to a similar possibility. It is therefore worth mentioning that the steel under study exhibited unusual combination of high ductility and work hardening rate. This helped in qualifying the material as suitable for reinforcement under conditions where welding is not mandatory.

During the analysis it was also revealed that the material exhibited two-stage hardening behaviour with 'n' values of 0.26 and 0.09 at different strain levels (Figure 3). The slope changed at a 'knee-strain' of ~0.05. A similar inference could be arrived at on observing the work hardening rate ($\partial\sigma/\partial\varepsilon$) versus true strain plot (Figure 4). The existence of a two-stage hardening can be attributed, mainly to the presence of microstructure consisting of a hard dispersed second phase in a softer matrix. The mechanism(s) explaining the 'double-n' effect in materials have been put forth in the past and different view points as to the likely reasons have emerged. Accordingly, hard phases in materials start yielding first giving rise to the first stage hardening. Second stage hardening can be attributed to the subsequent deformation experienced by the matrix. The presence of 'double-n' effect in materials is attributed to the existence of particle-matrix interface. A third view point is based on the formation of dislocation cells near to the grain boundaries as well as at phase boundaries.

In dual phase steels containing martensite (as harder phase) in a comparatively softer ferrite matrix during the initial stage(s) of plastic deformation, a high dislocation density exists adjacent to the grain boundaries and phase boundaries and this markedly increases internal stresses. Inhomogeneous deformation taken place in different grains within the matrix. As the deformation further increases, more and more grains are deformed, dislocation networks are formed and internal stresses increase gradually. During this process a stage reaches when strain differences among most of the grains and second phase particles are at a minimum. At this stage, dislocations causing multi-slip begin to cross slip and cells are formed. Dislocation densities and configurations are nearly similar in all grains, so that the internal stresses reach a transition critical value. This results in appearance of 'critical strain' or 'knee strain' [4] in the material. Above the critical strain the gliding distance of dislocations in a grain is reduced from the whole grain to a cell. In the meanwhile cross slip may allow dislocations to move around obstacles to reduce dislocation interactions and screw dislocations of opposite sign can annihilate one another by means of cross slip, and thus the extent of hardening decreases. This gives rise to the second stage of hardening.

In the experimental C-Mn steel pearlitic microstructure formed a composite comprising the softer ferrite matrix reinforced with comparatively harder carbide lamellae of cementite. The interface between these lamellae and ferrite could act as a potential site for the formation of dislocation substructures. As the strain increases gradually, dislocation cells are formed at these interfaces and the corresponding flow stress increases. A high value of strain hardening exponent of ~0.26 in the

experimental steel is an indication of these happenings. After the knee strain is reached at about 0.05 strain, dislocation networks coalesce and gliding distances between pearlitic lamellae reduce. This in turn reduces the work hardening of material giving rise to an exponent of about 0.09 which is much less than the one observed during the first stage. From the point of view of application, a two stage hardening in reinforcing steels is advantageous because it provides an opportunity to the designer for designing much safer allowable stress levels. This obviously decreases the risk factor in reinforced concrete structures.

In so far as attainment of hardness in the as-rolled material is concerned, very high values were not obtained. With an increase in carbon equivalent it varied between 257-294 Hv only since the carbon equivalent varied over a narrow range of 0.69-0.86. This ensured that the steel was adequately ductile. Due to this reason the 8 & 10 mm diameter wire rods could be bent around a mandrel of 3d through 180° without a crack being visible on the bent surface (Figure 5). Achieving 15-22 % elongation is another evidence of adequate formability / ductility in the steel. This is duly confirmed by perusing the fractographs summarized in Figure 6(b) wherein 100% dimpled fracture was observed in the wire rods even at carbon equivalents of upto 0.84.

5.0 Conclusions

Based upon the analysis of results and subsequent discussions on structure-property relationships in C-Mn steel wire rods the following conclusions were drawn.

1. The microstructure in as rolled state consisted of 80-93 % pearlite, the balance being grain boundary ferrite. Prior austenite grain size varied between 28-40 μm .
2. Through normal processing the steel achieved a yield strength of 422-585 MPa, UTS of 790-955 MPa, elongation of 15-22%, reduction in area 35-45% and hardness of 257-294 Hv. These values are in conformity with the requirements of Fe₄₁₅ grade reinforcement, as laid down in BIS:1786 specification.
3. In the as-rolled condition the material exhibited a two-stage work-hardening response indicating a different behaviour before and after a 'knee strain' of 0.05. The flow stress and strain were inter-related through the following model.

$$\begin{aligned}\sigma &= 1715\varepsilon^{0.26} && \text{for } \varepsilon \leq 0.05, \text{ knee strain} - 1^{\text{st}} \text{ stage hardening} \\ &= 1065 \varepsilon^{0.09} && \text{for } \varepsilon > 0.05, \text{ knee strain} - 2^{\text{nd}} \text{ stage hardening}\end{aligned}$$
4. UTS and hardness in the as rolled condition were linearly related through a relationship of the form: UTS (MPa) = 4.42 Hv - 354
5. Wire rods could be bent around a mandrel of 3d without any cracking being observed on the bent surface. This indicated adequate ductility and formability in the material and reflected favorably on the microstructure obtained. Presence of 100% dimples in the tensile fractured surface also confirms the same.

Acknowledgements

The authors are grateful to the management of RDCIS, SAIL for permitting presentation of this work in the conference.

References

- [1] Singh R K and Ramaswamy V, *Steel India*, vol II, No 1, (1988) p 34.
- [2] Duckworth W E, Phillips R and Chapman J A, *JISI*, Nov (1965) p 1108.
- [3] BIS:1786-1985; *Specifications for high strength deformed steel bars for concrete reinforcement*.
- [4] Atkinson M, *Met. Trans.*, vol 15A, June 1984 p 1185.
- [5] Ray K K and Mondal D, *Acta Met.*, vol 39, No.10 (1991), p 2201.
- [6] Gladman T and Pickering F B, *Flow and Fracture of Poly Crystals*, Applied Science, London, 1983.